International Journal of Control and Automation
Vol. 9, No. 9 (2016), pp.363-374
http//dx.doi.org/10.14257/ijca.2016.9.9.35

Design of Vibration Excitation Test Rig with Redundant Degree of Freedom

Shaobo Wen[1,*], Yu Zhang[1], Shuxin He[1] and Yunsong Lv[2]

[1]*School of Automotive and Rail Trait, Nanjing Institute of Technology, Nanjing 211167, P.R. China;*
[2]*School of Mechanical Engineering, Nanjing Institute of Technology, Nanjing 211167, P.R. China*
**. wenw2000@126.com*

Abstract

In order to provide controlled indoor experiment condition for the anti-vibration performance test of vehicle suspension, the multi-link vibration excitation test rig with redundant degree of freedom, which can simulate the different roughness roads and can produce stable, ergodic, random vibration excitation, was designed in the paper. First, according to the different redundant degrees of freedom, the four and three degrees of freedom vibration excitation test rig structural schemes were designed respectively, and the solid model and motion simulation of vibration excitation test rig were performed based on virtual technology, then the time history curves of displacement, velocity and acceleration at work bench were obtained. Second, vibration properties and characteristics of the two schemes were ascertained by using self-power spectral density, symbol time series histogram and Shannon entropy, thereby three degrees of freedom scheme was considered better on the basis of random vibration level and impact force of mechanism. Finally, acceleration root mean square of work bench was set as evaluation index of vibration excitation test rig's vibration excitation energy, and support distance, driven-crank rotation speed and spring stiffness under work bench were selected as influencing factors, then three factors and three levels of orthogonal design was conducted to determine three grades of vibration excitation test rig.

Keywords: *Redundant degree of freedom; Multi-link; Vibration excitation test rig; Virtual design; Orthogonal design*

1. Introduction

Since the profile of road has a stationary random roughness and Ergodic properties [1], road excitation is considered as random signal in ISO 2631 (1997) [2], the root mean square (RMS) of weighted acceleration and the vehicle ride comfort index are obtained by detecting the vibration acceleration at multiple seat parts, and they can be used to judge the effect of the anti-vibration performance of vehicle suspension to the vehicle ride comfort [3-4]. Inspected in accordance with the standard, larger experiment venues and different grade roads are required, and road surface irregularity, slope, straight length, degree of drying, weather condition, wind speed and other experimental conditions are difficult to be strictly controlled. Therefore, it has important practical significance to substitute indoor experiment for venues experiment.

When the anti-vibration performance of vehicle suspension is inspected in the indoor test rig, there are four excitation vibration methods at present, such as resonance method, press bodywork method, falling method and braking method, the essence of resonance method is sine sweep frequency stimulation, and other else are added an impulse

ISSN: 2005-4297 IJCA

excitation to the vehicle suspension [5]. Sine sweep excitation and impulse excitation are all different the actual road excitation on the vehicle suspension, so they cannot be used to accurately simulate the actual conditions of the road.

The dynamic equation of mechanism kinematic pair with clearance is nonlinear [6-7]. Even if the initial conditions and boundary conditions are determined, a range of random output would be obtained for the nonlinear equations. But motion parts with clearance will cause large impact and wear between each other, and quicken the fatigue failure of parts [8]. Based on this reason, a multi-link slider vibration mechanism with redundant degree of freedom (DOF) is established to substitute for kinematic pair with clearance. The reciprocating motion of the mechanism with random vibration characteristics can be used to simulate the excitation that the vehicle suspension is motivated by the road.

2. Modeling of Mechanism

Vehicle suspension vibration test rig based on multi-link mechanism is designed according the above idea, and the basic schematic diagram is shown in Figure 1. The mechanism has four DOF, called as 4DOF scheme. The original driving crank OA rotates at a constant speed ω, then plane motion is realized by link AB, multi-node link BCD, link CF, link FG and slider W; the reciprocating motion at slider W would have the characteristics of random vibration.

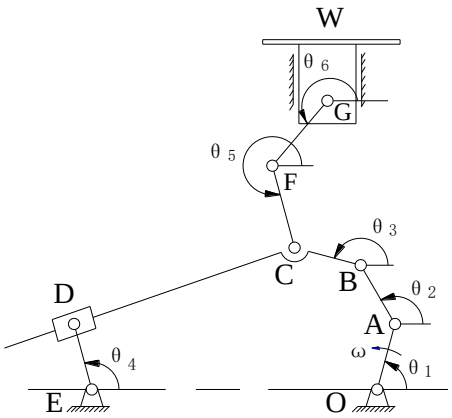

Figure 1. Schematic Diagram of 4DOF Vibration Excitation Test Rig

If link CF and link FG are merged into one link CG, the DOF of mechanism is changed to three, so it is called as 3DOF scheme.

Comparing to kinematic pair with clearance, a relatively little shock and wear of mechanism will occur by multi-link mechanism with redundant DOF, and it can prolong life of mechanism.

3. Virtual Design of Vibration Test Rig

Since the excitation test rig has redundant DOF, analytical solution of the kinematic parameter at the slider W can not be obtained directly [9]. In the paper, virtual prototype design of multi-link vehicle suspension excitation test rig is performed by computer-aided design.

3.1. Modeling Vibration Test Rig

According to the schematic diagram of 4DOF vibration test rig, three-dimensional solid modeling and virtual assembly of mechanism parts are conducted in UG software. Virtual assembly drawing of the vibration test rig is shown in Figure 2.

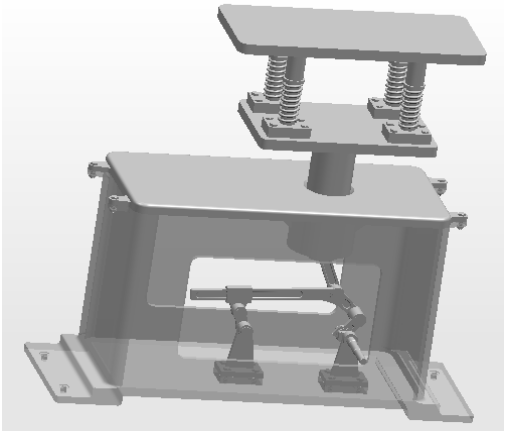

Figure 2. Model of Vibration Excitation Test Rig

When the three-dimensional model of 4DOF scheme is establishing, the link FG (as shown in Figure1) is designed as a shaft with small gyration radius. The gyration radius of link FG is designed as a variable parameter by parametric modeling characteristics in UG software, when its value is 0, the scheme is degenerated into 3DOF. In addition, in order to acquire more fragmented output at work bench, four springs with constant stiffness are set between slider W and work bench, as shown in Figure 2.

3.2. Motion Simulation Analysis of Vibration Test rig

The motion data of mechanism model can be obtained based on kinematic analysis module in UG software, and the results can be applied to guide the parts design.

3.2.1. Determining the Main Dimension

Dimensions of main parts is determined by joint motion. Joint motion is on the bases of the displacement of driving part, it is determined by the driving step length and the step number of driving part. For an excitation amplitude is given as $\pm$ 75 mm at work bench and spring stiffness under the work bench is set as 1.25×105 N/m, the main parts dimensions of the mechanism for 4DOF scheme are shown in Table 1. If FG = 0, the mechanism is degenerated as 3DOF scheme.

Table 1. Principal Dimension of 4DOF Vibration Excitation Test Rig

Main part	OA	AB	BC	DE	CF	FG	OE
Dimension, mm	13	60	68	42	148	2.2	280

3.2.2. Motion Simulation

Motion simulation is a kind of motion form based on time. If motion form, time and velocity of driving part are conformed, the motion data of mechanism can be analyzed in the period.

The rotation speed of driving crank OA is set as 360 rpm, and running time is 8 second, motion data at vibration work bench is exported. For the two schemes of vibration excitation test rig, displacement, velocity and acceleration curve at work bench are shown in Figure 3 to Figure 5.

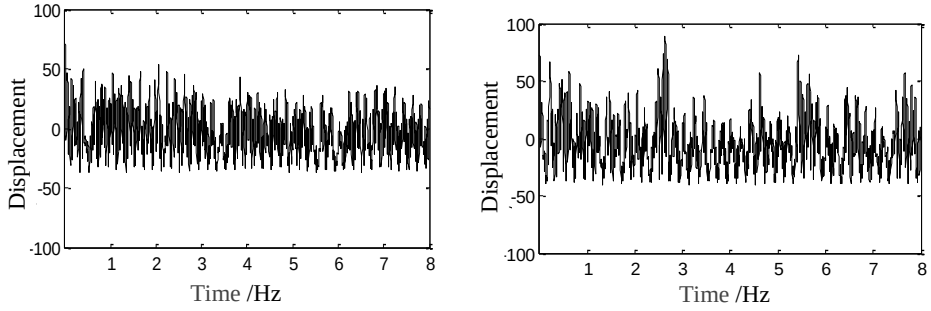

(a) 3DOF scheme (b) 4DOF scheme

Figure 3. Displacement Time History Curve at Vibration Work Bench

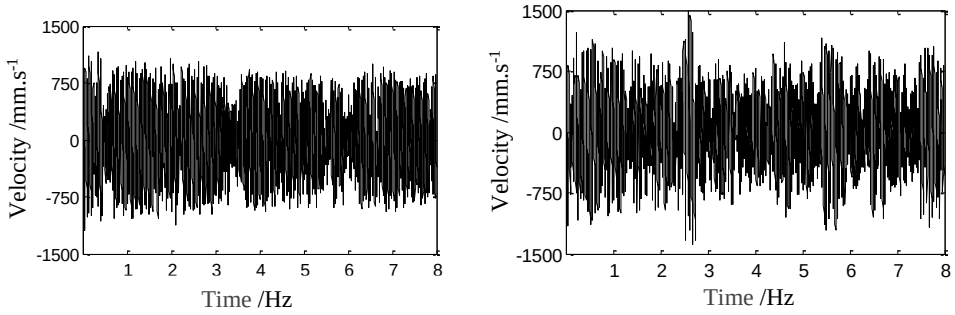

(a) 3DOF scheme (b) 4DOF scheme

Figure 4. Speed Time History Curve at Vibration Work Bench

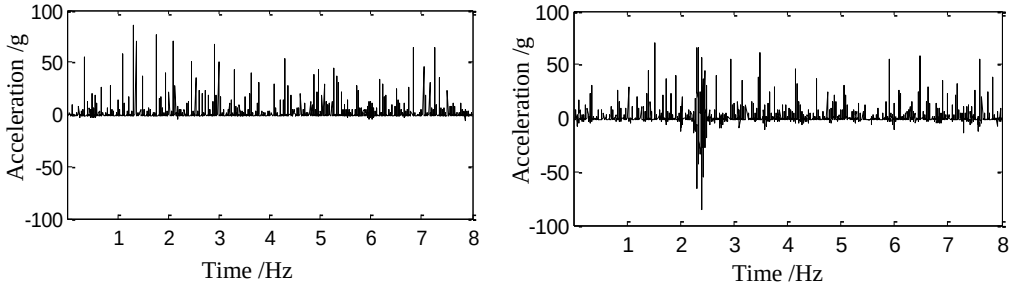

(a) 3DOF scheme (b) 4DOF scheme

Figure 5. Acceleration Time History Curve at Vibration Work Bench

From Figure 3 to Figure 5:

In the aspect of vibration characteristics, redundant DOF of vibration excitation test rig have great effect on vibration output at work bench, its motion has lost cyclical of original driving crank OA.

In the aspect of vibration value, different DOF of vibration test rig have different effect on vibration output at work bench. For 3DOF scheme, acceleration range is -5g~85g, intermediate value is 45g; as for 4DOF scheme, acceleration range is -86g~66g, intermediate value is 76g. The vibration value of latter is bigger than that of former.

Disorder properties of acceleration at work bench in the two schemes are similar that of mechanism with clearance [10-11], so the mechanism with redundant DOF replace mechanism with clearance is feasible.

4. Vibration Characteristics Analysis at Work Bench

While vibration acceleration at work bench has completely lost motion periodicity of original driving part as shown in Figure3 to Figure5, but if want to make sure the vibration properties and characteristics, we also need to adopt other appropriate approaches. In the study, self-power spectral density, symbolic time series histogram and Shannon entropy are adopted to determine vibration properties, characteristics and the randomness degree of 4DOF and 3DOF scheme.

4.1. Self-Power Spectral Density Analysis

By investigating the frequency composition and distribution of time series in discrete frequency domain, we can identify aperiodicity, periodicity or randomness of time series. The periodic time series have discrete and equal interval frequency spectrum, the aperiodic time series have discrete and unequal interval frequency spectrum, and the random time series have discrete, unequal interval and inseparable frequency spectrum [12]. Self-power spectral density can simultaneously reflect frequency composition and distribution of time series in frequency domain, so it can be used to examine vibration properties and characteristics of acceleration time series at work bench.

When the sampling frequency is more than twice of the highest signal frequency, the original signal spectrum and additional spectrum is not overlap, then the original signal frequency spectrum can be extracted from sampled signal spectrum [13, 14]. In the study, 128 Hz frequency is used to sample acceleration data at work bench, then 0~64 Hz frequency of vibration frequency distribution and its characteristics can be obtained.

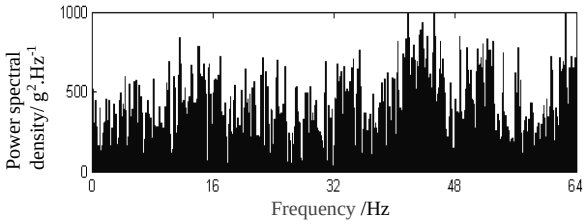

(a) 3DOF scheme

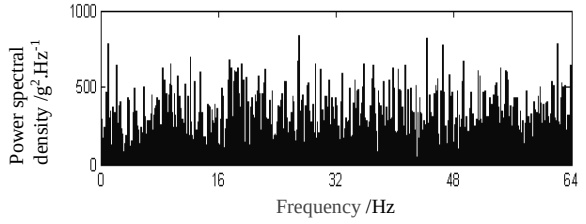

(b) 4DOF scheme

Figure 6. Vibration Acceleration Time Series Self-Power Spectral Density at Vibration Work Bench

Time series self-power spectral density of vibration acceleration at work bench is shown in Figure 6. As can be seen in Figure 6, self-power spectral density of two schemes are discrete, unequal interval and inseparable, vibration of two schemes can be regarded as random vibration.

4.2. Symbolic Time Series Histogram and Shannon Entropy Analysis

Symbolic time series histogram and Shannon entropy can be used to describe the data disorder-random level. For completely random time series, each probability of amplitude is equal. Any large probability of amplitude is corresponded to a deterministic structure. Distribution of symbolic time series histogram probability is more uniform, the randomness of the time series is stronger. Symbolic time series histograms of vibration acceleration at work bench are shown in Figure 7.

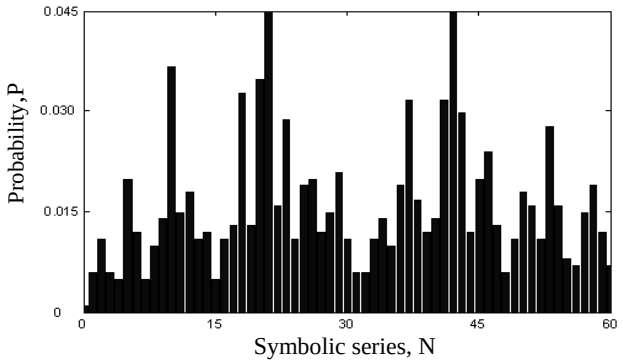

(a) 3DOF scheme

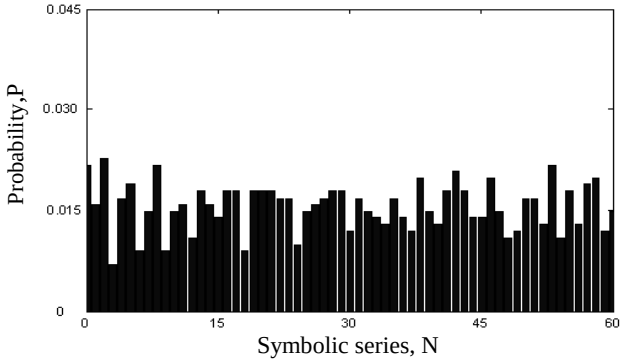

(b) 4DOF scheme

Figure 7. Acceleration Symbolic Time Series Histograms at Vibration Work Bench

Shannon entropy can be obtained by symbolic time series histogram [15]. According to binary symbolic rule, Shannon entropy is defined as

$$H_s(L) = -\frac{1}{L\ln 2}\sum p_{s_1 s_2 \cdots s_L} \ln\left(p_{s_1 s_2 \cdots s_L}\right) \quad (1)$$

where, L is the length of short symbolic series, $p_{s_1 s_2 \cdots s_L}$ is the probability corresponding to each symbolic series in the histogram.

Shannon entropy values of completely random time series and deterministic time series are 1 and 0, respectively. It is possible to determine the degree of randomness of time series by comparing the value of Shannon entropy. After data acquisition from Figure 5, for the two schemes, the symbol probability variance and the Shannon entropy of the vibration acceleration at work bench can be obtained, as shown in Table 2.

Table 2. Symbolic Parameter of Two Schemes of the Vibration Excitation Test Rig

	Symbol probability variance	Shannon entropy
4DOF	1.2215×10-5	0.9938
3DOF	9.3663×10-5	0.9591

Analysis showed that by observing Figure 7 and Table 2, the symbolic time series histogram probability of two schemes are uniform distribution, Shannon entropy values are all close to 1, so the vibration of two schemes at work bench are treated as random vibration. In addition, comparing to 3DOF scheme, symbol probability variance of 4DOF scheme is smaller, symbolic time series histogram probability distribution is more uniform, and Shannon entropy value is greater, so degree of randomness of 4DOF scheme is stronger.

5. Comparison of Two Excitation Test Rig Schemes

A load of 500kg (about one-quarter weight of a medium car) is added at work bench, and dynamics calculation is conducted to reversely determine each joint force of the test rig. The instantaneous maximum impact force of each joint can be obtained, and these can be used as a basis for checking the strength of each link.

As for the two schemes, the maximum impact force of each joint, the vibration acceleration range, intermediate value, Shannon entropy at work bench are listed in Table 3 (each joint point label are correspond to the letters of Figure 1).

Table 3. The Impact Force and Acceleration of Two Schemes of the Vibration Excitation Test Rig

Scheme	Maximum impact force of each joint, N					Acceleration at work bench		
	A	B	C	D	G	range	intermediate value	Shannon entropy
4DOF	107293	107286	80933	106227	80331	-86 g ~ 66 g	76 g	0.9938
3DOF	72485	72186	70671	23847	70157	-5 g ~ 85 g	45 g	0.9591

Table 3 can be analyzed as follows:

(a) The maximum impact force of each joint of 4DOF scheme is much bigger than that of 3DOF scheme, for example, the value of former is 4.5 times than that of the latter in D joint, indicating that mechanism parts of 4DOF scheme suffered greater load.

(b) Acceleration intermediate value at work bench of 4DOF scheme is bigger than that of 3DOF scheme, indicating impact of 4DOF scheme is greater than that of 3DOF scheme under work station.

(c) Although the Shannon entropy value of 4DOF scheme is greater than that of 3DOF scheme, but the difference between the two schemes is only 3.5%, indicating the randomness of the former is slightly stronger than that of the latter.

Based on the above analysis, the two excitation test rig schemes also can realize random vibration, and the difference of randomness degree is small, but difference of load and impact on the mechanism parts is huge. Comparing to 4DOF scheme, 3DOF scheme has the advantages of simple structure and less impact force, so it is recommended to use in the paper.

6. Orthogonal Design of 3DOF Excitation Test Rig

6.1. Performance Evaluation of Test Rig

In order to properly judge the effectiveness of the excitation test rig and design optimization, it is need to analysis excitation energy under work station, and excitation acceleration RMS value is used as the evaluation criteria in the study.

Virtual experimental design, simulation run mechanism, acceleration time history curve is output in UG software. Based on the sampling theorem, the RMS value of acceleration at work bench is obtained as evaluation index, and it is seen in Equation (2) as follows [16]. The RMS of acceleration is greater, the excitation energy is greater.

$$y = \sqrt{\frac{\sum_{i=1}^{N}\left(a_i - \overline{X}\right)^2}{N-1}} \tag{2}$$

where, y is the acceleration RMS value of data sample, N is the sample number, i is series number of data acquisition, a_i is the acceleration data sample of the test rig, $\overline{X}$ is the mean value of the sample data.

6.2. Orthogonal Experimental Design

For excitation test rig of 3DOF scheme above recommended, excitation energy is used as evaluation index under work station, spacing distance OE, drive crank speed, spring stiffness under work bench are chosen as influence factors, virtual orthogonal experiment is conducted.

Firstly, according to dimension requirements of excitation test rig, rotation speed range of DC motor and natural frequency range of vehicle suspension, the internal levels and factors are analyzed preliminary. Spacing distance, drive crank rotation speed, spring stiffness are set three levels, experimental factors and levels are shown in Table 4.

Table 4. Factors and Levels of Orthogonal Experiment

Levels	Factors		
	A	B	C
	Support distance (mm)	Driven-crank rotation speed (rpm)	Spring stiffness (10^5 N/m)
1	320	360	0.8
2	280	540	1.25
3	240	720	1.8

For the orthogonal experimental scheme of three levels and three factors, it can be used L9(3^3) experimental scheme [17-18]. The experimental scheme and results are shown in Table 5.

Table 5. Orthogonal Design L9 (33) and Results of Orthogonal Experiment

No.	Factors			RMS of the acceleration y (m/s^2)
	A	B	C	
1	1	1	1	28.861
2	1	2	2	35.899
3	1	3	3	46.138
4	2	1	2	67.984
5	2	2	3	62.089
6	2	3	1	43.411
7	3	1	3	62.034
8	3	2	1	69.737
9	3	3	2	72.059

6.3. Orthogonal Experimental Results

Orthogonal experimental results are shown in Table 6. Range (as seen in Equation (3)), which is the difference of experimental results between maximum and minimum of each level of a factor, is usually used to measure the affect of factors in orthogonal experiment analysis. Generally, range of each column is not equal, that is to say, the influence of each factor on the experimental results are different.

The range value of a factor is greater; the affect of the factor to the experiment is greater.

$$R = \max\{t_1, t_2, t_3\} - \min\{t_1, t_2, t_3\} \quad (3)$$

where, R is range, $\max\{t_1, t_2, t_3\}$ and $\min\{t_1, t_2, t_3\}$ are the maximum value and the minimum value of the corresponding column in Table 6, respectively.

Table 6. Orthogonal Experiment Results Analysis

	A	B	C
Total RMS at level 1, T_1 (m/s^2)	110.898	158.879	142.009
Total RMS at level 2, T_2 (m/s^2)	173.484	167.725	175.942
Total RMS at level 3, T_3 (m/s^2)	203.830	161.608	170.261
Mean RMS at level 1, t_1 (m/s^2)	36.966	52.960	47.336
Mean RMS at level 2, t_2 (m/s^2)	57.828	55.908	58.647
Mean RMS at level 3, t_3 (m/s^2)	67.943	53.869	56.754
Range R (m/s^2)	30.977	2.948	11.311
Optimal level	A_3	B_2	C_2
Effect order of Factors	A C B		

As listed in Table 6, range of factor A (support distance) is biggest, so the affect of the factor A to the experiment is maximum, range of factor B (driven-crank rotate speed) is minimal, and range of factor C (spring stiffness) is medium.

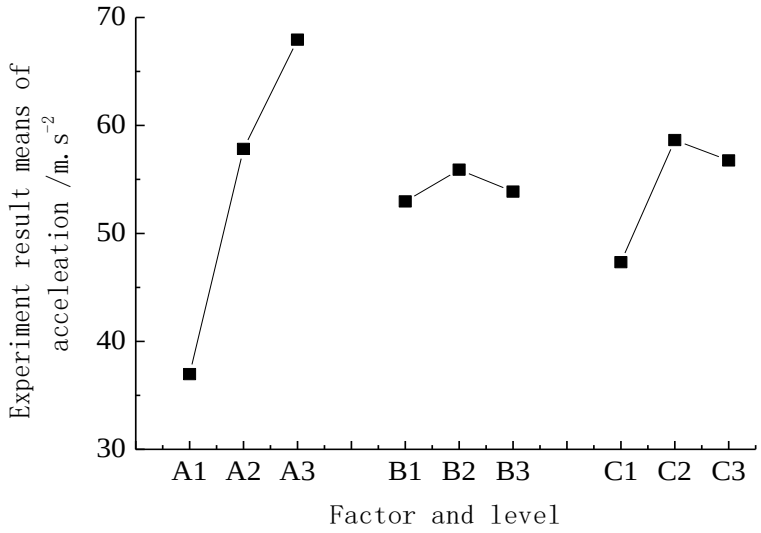

Figure 8. Effects of Factors and Levels

In the study, the trend of effects of factors and levels is shown in Figure 8. As can be obtained from Figure 8, the closer support spacing will increase the RMS of the acceleration at work bench in the whole range of constraints, so A3 is the optimal level. While increasing rotation speed of drive crank and spring stiffness, the RMS of the acceleration will firstly increase and then decrease.

Based on the evaluation criteria of excitation energy, if want to achieve the maximum excitation energy, support spacing should be selected closer (level 3), driven crank rotation speed and spring stiffness should be selected moderate (level 2), it can be written as $A_3B_2C_2$ scheme; similarly, the medium energy scheme and the minimum energy scheme are $A_2B_3C_3$ and $A_1B_1C_1$, respectively.

Scheme $A_1B_1C_1$ has been calculated in the orthogonal experiment, the results can be obtained directly from Table 5. The schemes $A_3B_2C_2$ and $A_2B_3C_3$ does not appear in the orthogonal experiments, respectively, acceleration data of them are acquired according to motion simulation, and then the RMS of the acceleration can be calculated, the results are shown in Table 7.

Table 7. Vibration Energy Comparison of Different Grades

	Low-grade: $A_1B_1C_1$	Middle-grade: $A_2B_3C_3$	High-grade: $A_3B_2C_2$
RMS of vibration acceleration (m/s^2)	28.861	49.812	72.442
The excitation energy range	58%	100%	145%

As can be seen from Table 7, vibration acceleration RMS values of the low-grade, mid-grade and high-grade at work bench are 28.861 m/s^2, 49.812 m/s^2 and 72.442 m/s^2, respectively. Excitation energies of low-grade and high-grade are about 58% and 145% that of mid-grade, respectively, the energy output of different grades are obvious.

So excitation test rig based on excitation energy output are set three grades, low-grade is $A_1B_1C_1$, mid-grade is $A_2B_3C_3$ and high-grade is $A_3B_2C_2$.

7. Conclusions

A multi-link vehicle suspension excitation test rig, which can simulate different road roughness and produce stable, ergodic random vibration excitation, is designed for the anti-vibration performance test of vehicle suspension in indoor experiment conditions.

(1) Accordance to the multi-link motion principle, two schemes (4DOF and 3DOF) of vehicle suspension excitation test rig is established. Based on virtual prototype technology, three-dimensional solid modeling, virtual assembly and motion simulation of excitation test rig are performed in UG software, time history curves of displacement, velocity and acceleration at vibration work bench are obtained.

(2) The vibration characteristics of 4DOF and 3DOF scheme are determined by self-power spectral density function, symbolic time series histogram and Shannon entropy, and then the 3DOF scheme of excitation test rig is selected as a better scheme according the randomness degree of vibration and impact force on the mechanism.

(3) The acceleration RMS value of vibration excitation at work bench is selected as evaluation index, the support distance, driven crank rotation speed and spring stiffness under work bench are set as influence factors, the three factors and three levels of virtual orthogonal experiment are conducted, then three grades of excitation test rig is identified.

Acknowledgements

This work was supported by Nanjing Institute of Technology Science Fund (ZKJ201506) and (CKJB201216), Jiangsu Province Natural Science Fund (BK2012866) and National Science Fund of China (51405221).

References

[1] J.D. Robson and C.J. Dodds, “Stochastic road inputs and vehicle response”, Vehicle System Dynamics, vol.5, no.1-2, **(1976)**, pp.1-13.
[2] ISO, “Mechanical vibration and shock-Evaluation of human exposure to whole-body vibration-Part 1: General requirements”, International Organization, **(1997)**.
[3] G.S. Paddan and M.J. Griffin, “Evaluation of whole-body vibration in vehicles”, Journal of Sound and Vibration, vol. 253, no.1, **(2002)**, pp.195-213.
[4] P. Mucka and O. Kropac, “Properties of random component of longitudinal road profile influenced by local obstacles”, International Journal of Vehicle Systems Modeling and Testing, vol.4, no.4, **(2009)**, pp.256-276.
[5] J.H. Lee and W.S. Yoo, “An improved model-based predictive control of vehicle trajectory by using nonlinear function”, Journal of mechanical science and technology, vol.23, no.4, **(2009)**,pp.918-922.
[6] K. Soong and B.S. Thompson, “A theoretical and experimental investigation of the dynamic response of a slider-crank mechanism with radial clearance in the gudgeon-pin joint”, Journal of Mechanical Design, vol.112, no.2, **(1990)**, pp.183-189.
[7] S. Erkaya and I. Uzmay, “Investigation on effect of joint clearance on dynamics of four-bar mechanism”, Nonlinear Dynamics, vol.58, no.1-2, **(2009)**,pp.179–198.
[8] J.F. Deck and S. Dubowsky. “On the limitations of predictions of the dynamic response of machines with clearance”, Journal of Mechanical Design, vol.116, no.3, **(1994)**, pp.833~841.
[9] K. Hu, Z.P. Mourelatos and N.Vlahopoulos, “Computational analysis for dynamic response of a rotating shaft on flexible support structure with clearances”, Journal of sound and vibration, vol.267, no.1, **(2003)**, pp.1-28.
[10] I. Khemili and L. Romdhane, “Dynamic analysis of a flexible slider–crank mechanism with clearance”, European Journal of Mechanics-A/Solids, vol.27, no.5, **(2008)**, pp.882-898.
[11] S. Erkaya and İ.Uzmay, “Experimental investigation of joint clearance effects on the dynamics of a slider-crank mechanism”, Multibody system dynamics, vol.24, no.1, **(2010)**, pp.81-102.
[12] J.S. Bendat and A.G. Piersol, “Random data: analysis and measurement procedures”, John Wiley & Sons Inc. (**2011**).

[13] K. Kim, I.A. Akbar, K.K. Bae, U. JungSun, C.M. Spooner and J.H. Reed, "Cyclostationary approaches to signal detection and classification in cognitive radio", New frontiers in dynamic spectrum access networks, 2nd IEEE international symposium on. IEEE, **(2007)**, April 17-20, Dublin, Ireland.
[14] J. Antoni and R.B. Randall, "The spectral kurtosis: application to the vibratory surveillance and diagnostics of rotating machines", Mechanical Systems and Signal Processing, vol.20, no.2, **(2006)**,pp.308-331.
[15] S. Gupta, A. Ray and E. Keller, "Symbolic time series analysis of ultrasonic data for early detection of fatigue damage", Mechanical Systems and Signal Processing, vol.21, no.2, **(2007)**, pp.866-884.
[16] R.S. Figliola and D.E. Beasley, "Theory and design for mechanical measurements", John Wiley & Sons Inc. **(2001)**.
[17] M. Kurt, E. Bagci and Y. Kaynak, "Application of Taguchi methods in the optimization of cutting parameters for surface finish and hole diameter accuracy in dry drilling processes", The International Journal of Advanced Manufacturing Technology, vol. 40,no.5-6, **(2009)**,pp. 458-469.
[18] P. Sharma, A. Verma, R.K. Sidhu and O.P. Pandey, "Process parameter selection for strontium ferrite sintered magnets using Taguchi L9 orthogonal design", Journal of materials processing technology, vol.168, no.1, **(2005)**,pp. 147-151.

